Ambient seismic noise tomography in the Lake Toba region, Indonesia

Jacek Stankiewicz, Trond Ryberg, Christian Haberland, Michael Weber

Helmholtz Centre Potsdam
GFZ German Research Centre for Geosciences

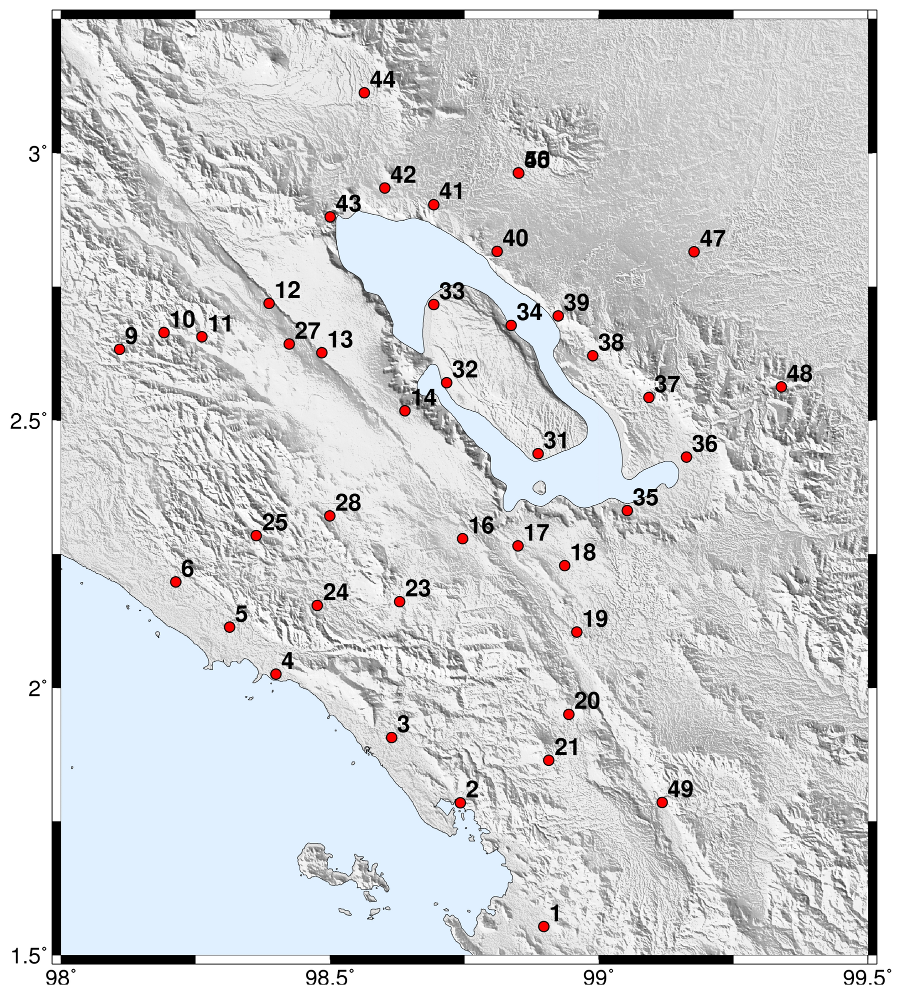

INTRODUCTION

The Toba caldera in located in north Sumatra, Indonesia. It is part of the volcanic arc associated with the subduction of the Australian Plate beneath the Southeast-Asian Plate. The caldera is known as the location of one of the largest Quarternary caldera on Earth, formed 75ka ago by an eruption of 2500-3000km³ of material. This volcanic event had a significant global impact on climate and the biosphere. The presence of a magma reservoir beneath the Toba caldera has been revealed by previous geophysical analysis that relied on an inversion of P-wave arrival times and gravity anomalies. The goal of our seismic studies carried out in 2008 is to understand the present-day magma distribution by high resolution mapping of crustal seismic velocities tomographically derived from ambient noise records.

Between May and October 2008, a dense seismic network was installed around Lake Toba (Fig. 1). The network comprised of 40 continuously recording seismic stations. They were equipped with three-component, short-period seismic sensors with 1Hz natural frequency. The GPS synchronised data loggers recorded at 100 samples per second for the experiment's time span of 6 months. During this time period local and regional seismicity was recorded. Although short-period sensors were used, there was significant strong noise energy in the 0.06 to 1 Hz frequency band, which formed the base for an ambient noise tomography study.

METHOD

The idea of extracting coherent signal by cross-correlation of noise has its roots in helioseismology. Recently it was suggested that Rayleigh waveforms can be recovered from cross-correlating vertical components of seismic noise recorded simultaneously at two or more stations. The method used in this study involves calculating the cross-correlation integral for the daily time series records for all available station pairs in the 50 station array. For stations A and B, this integral of the stations' individual time series, *z*, is given as: $G(A,B,t)=\int_{-\infty}^{\infty} z(A,\tau)z(B,\tau+t)d\tau$

For each available station pair, the resulting correlation function, *G*, is a two sided time function with both positive and negative correlation lags. While each correlation is twice as long as the input files, i.e. two days, given a maximum station distance of 177 km it was sufficient to store the sections from -150 to 150 seconds. The daily correlation functions were stacked for each station pair to improve the signal to noise ratio. Emergence of signal can be seen in the correlations of records from station 4 with all other static

a) single day b) 10 day stack c) all available days

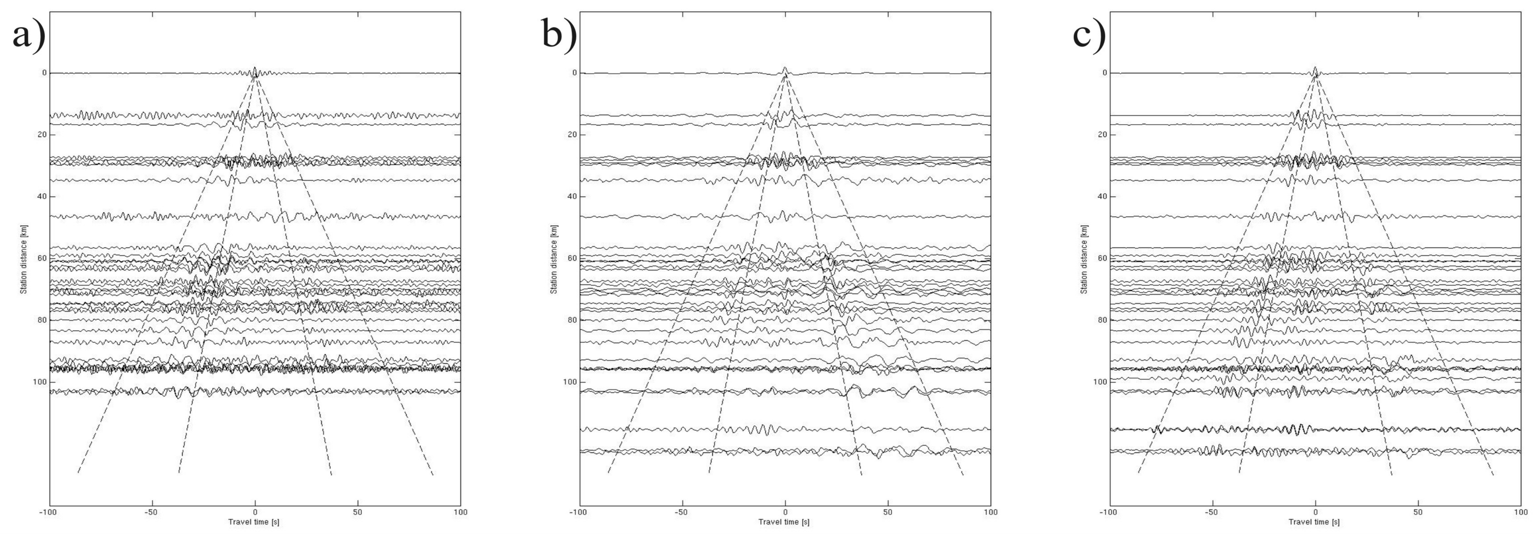

PROCESSING

After stacking the daily records, the arrival times of Rayleigh waves were calculated. As surface wave velocities are frequency dependent, this was done using the frequency-time analysis. Each Green's function was filtered with progressively higher period range, and the envelope of each resulting filtered trace was calculated. The peaks of these envelopes was then traced across the spectrum. Separate dispersion curves were drawn for the two propagation direction – these often contained energy at different frequencies. This impies energy arriving from different directions at different frequencies. Example below shows the signal between stations 4 and 12.

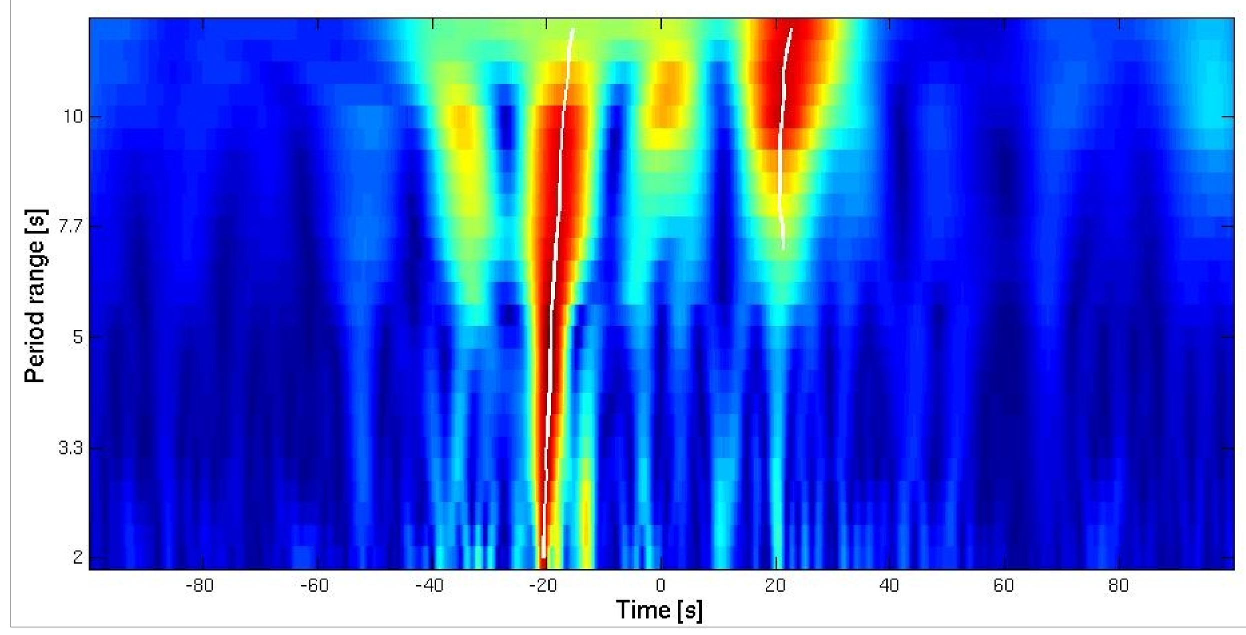

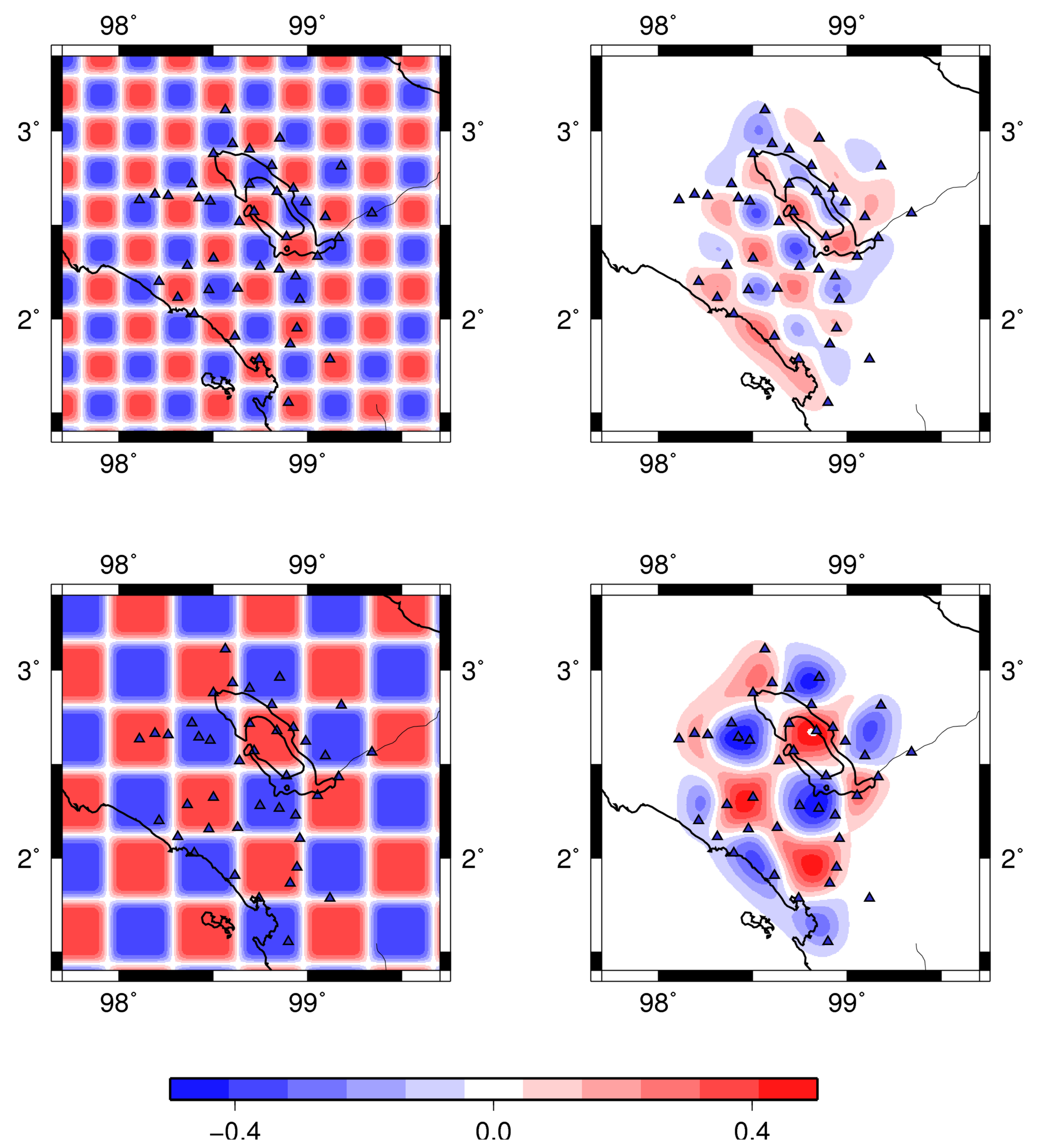

RESOLUTION

The final velocity models for different period ranges were each calculated on a 2° by 2° grid, separated into 30 nodes in each lateral direction. These are shown on the right. To investigate their resolution, checkerboard tests were performed. The quality of the recovered patterns gives an indication of the size and location of resolvable features.

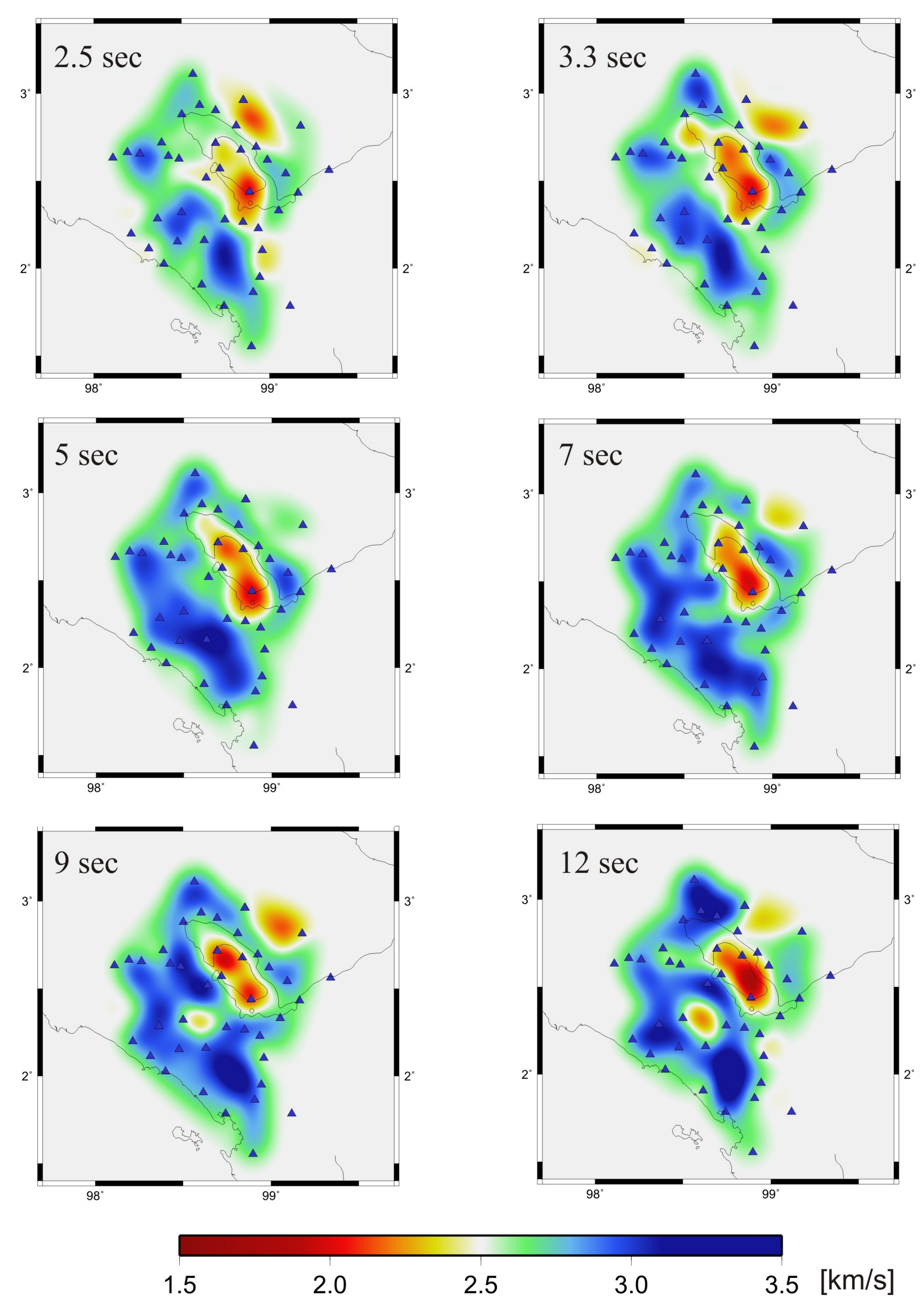

DISCUSSION AND CONCLUSIONS

Rayleigh waves have frequency dependent group velocities due the fact that different frequencies sample different depths. High frequency (short period) waves penetrate only the shallow sub-surface, while low frequency (long period) waves penetrate deeper into the crust. The 2.5 second signal samples the uppermost 2-3 km, while the 12 second signal can reach down to 10-15 km.

Having obtained Rayleigh wave travel times between station pairs for a given period, a 2D tomographic inversion was performed to estimate variations in surface wave group velocities in the study area. The Fast Marching Surface Tomography (FMST) code developed by N. Rawlinson was used. The resulting 2D velocity models show the lateral variations in Rayleigh wave velocities averaged between the surface and the sampling depth of the given frequency.

One of the most prominent features of all velocity model shown in Fig. 4 is the low velocity zone coinciding with the location of Lake Toba and the caldera island. High temperatures are responsible for reduced seismic velocities, so this zone is likely to correspond to the magma chamber underneath the volcanic island. The exact geometry of the magma chamber appears to be complex. While the lowest velocities are observed beneath the southern part of Samosir island, in some models a second low velocity region is clearly seen underneath the northern part of the island. While Toba is often referred to as a caldera, gravity and paleomagnetic studies suggest it is in fact a complex of several calderas. Our study show the caldera can in fact be separated into two distinct parts. The size of these parts is close to the resolving capabilities of our velocity models, making it impossible for us to state whether these are are single calderas or merely sub-complexes.

A significant feature is the low velocity zone south-west of the Lake present in the 12 seconds period model. It can also be seen, though less prominently, in the 9 and 7 seconds models. The size of this anomaly is definitely within the resolving capabilities of the inversion, and it is interpreted here as another magmatic body, extending from a depth of ~7 km downwards.

At lower periods (shallow depth, down to ~ 5 km), the Sumatra Fault marks a significant shift in velocity, with high velocities south-west of the Fault. However, the presence of the aforementioned low-velocity body, as well as high velocity zones present to the north of the lake, demonstrate that the simple bimodal velocity model defined by the Sumatra fault is not appropriate, and the tectonics in the region are much more complex.

We acknowledge the support of Danny Natawidjaja (Indonesian Institute of Science) and Fauzi Fauzi (Meteorological and Geophysical Agency, Indonesia) for their collaboration in this project. Furthermore we thank Bambang Suwargadi, Hendra Suwarta and all field crews for their excellent work under difficult conditions, and the landowners for hosting our stations. The seismic instruments were provided by the Geophysical Instrument Pool Potsdam. Funding for the experiments was provided by the GeoForschungsZentrum Potsdam. We thank Nick Rawlinson (ANU) for making his tomography code available to us. JS is funded by the Helmholtz-Russia Joint Research Groups (project HRJRG-110).